Economic Geology, v. XXX, no. XX, pp. X–X

Two Decades of Monitoring Hydrothermal Plumes at the Brothers Submarine Volcano, Kermadec Arc, New Zealand

Sharon L. Walker[1,†] and Cornel E.J. de Ronde[2]

[1] *Pacific Marine Environmental Laboratory, National Oceanic and Atmospheric Administration, 7600 Sand Point Way NE, Seattle, Washington 98115-6349, USA*

[2] *GNS Science, 1 Fairway Drive, Avalon, P.O. Box 30-368, Lower Hutt 6315, New Zealand*

Abstract

Brothers volcano is arguably the most well-studied submarine arc volcano on Earth. Between 1996, when massive sulfides were first recovered by dredging, and 2018, when International Ocean Discovery Program (IODP) Expedition 376 recovered cores from as deep as 453 m below the sea floor at two chemically distinct hydrothermal upflow zones, over 60 conductivity-temperature-depth (CTD) vertical casts and tow-yo operations mapped hydrothermal plumes over and around the edifice by employing hydrothermal tracer-specific sensors. These surveys started in 1999 and were completed during nine separate expeditions at one- to three-year intervals, except for a six-year gap between 2011 and 2017. Hydrothermal plume distributions over this two-decade period show variability in the intensity and vertical rise height of plumes from the four main vent fields (Upper Cone, Lower Cone, NW Caldera, and Upper Caldera, with the latter not discovered until 2017). Upper Cone plumes were more intense than all other sites in 1999, 2002, 2007, and 2009, then significantly diminished from 2011 to 2018. The Lower Cone plume was the most intense in 2004, then the NW Caldera site became the dominant source of hydrothermal particles from 2011 to 2018. Despite the gap of six years between 2011 and 2017, hydrothermal output appears to have increased within the caldera sometime after the 2009 survey while simultaneously decreasing in intensity at the cone sites. This supports other evidence of linkages between the cone and caldera sites in the deep hydrothermal circulation system, and may be related to the predicted deepening of hydrothermal circulation, infiltration of seawater to facilitate "mining" of magmatic brines, and modulation of subseafloor mineralization processes associated with a modeled, pulsed injection of magmatic gasses. The surveys also revealed ways in which the highly variable regional hydrographic environment impacts the flux of hydrothermal products to the surrounding ocean. Plumes from sources located above the caldera rim disperse hydrothermal components without hindrance, but particles and heat from sources within the caldera become trapped and are dispersed episodically by caldera-flushing events. While on site for 18 days in 2018, repeat CTD casts into the deepest part of the caldera, which was isolated from the surrounding ocean, showed a progressive increase in temperature, representing a net heat flux of 79 MW from conductive and advective sources deeper than 1,570 m.

Introduction

Brothers submarine volcano, located along the intraoceanic Kermadec arc about 400 km northeast of New Zealand (Fig. 1A), has been intensively investigated since it was first mapped and volcanic massive sulfides were obtained by dredging in 1996 (Wright et al., 1998; de Ronde et al., 2003), making it one of the most well-studied submarine arc volcanoes on Earth. In addition to mapping and dredging, studies have included sea-floor camera surveys (Stoffers et al., 1999; Clark and O'Shea, 2001; de Ronde et al., 2003, 2005), hydroacoustic monitoring (Dziak et al., 2008), dives with both manned submersibles and remotely operated vehicles (ROVs) to obtain samples of rocks, mineral deposits, vent fluids, and micro- and macrobiology (Stott et al., 2008; Takai et al., 2009; de Ronde et al., 2011; de Ronde and Stucker, 2015; Kleint et al., 2019; Diehl et al., 2020; Reysenbach et al., 2020), modeling studies (Gruen et al., 2012, 2014), magnetization and heat flux surveys (Caratori Tontini et al., 2012, 2019), and, most recently, International Ocean Discovery Program (IODP) Expedition 376, which drilled into the edifice to a maximum depth of 453 m below the sea floor within the upflow zones of two chemically distinct hydrothermal fields (de Ronde et al., 2019a, b; other studies included in this volume).

Early studies (i.e., camera surveys in 1998) first identified the northwest quadrant of the caldera (NW Caldera) and the shallower resurgent cone (Upper Cone) as sites with active hydrothermal venting (Fig. 1B; de Ronde et al., 2003). Subsequently, water column surveys during nine expeditions between 1999 and 2018 mapped the intensity and distribution of hydrothermal plumes at the edifice scale (Fig. 2). Hydrothermal plumes represent the integrated output from vent fields, and notably, the first such survey in 1999 showed that widespread neutrally buoyant hydrothermal plumes with distinct chemical signatures were dispersing at different depths, indicating the initially identified active sites (i.e., NW Caldera and Upper Cone) were extensive, emitted fluids with different compositions, and vigorously supplied hydrothermal heat and chemicals to both the water trapped within the caldera and the surrounding ocean (de Ronde et al., 2001; Baker et al., 2003; Massoth et al., 2003). The surveys in 2004 and 2005 showed significant plumes were also being generated at the deeper resurgent cone (Lower Cone). The physiochemical character of these plumes suggested that venting from this location was similar to emissions from the Upper Cone. Direct observations during manned submersible dives confirmed that the style of

[†]Corresponding author: e-mail, Sharon.L.Walker@noaa.gov

ISSN 0361-0128; doi:10.5382/econgeo.4998; 13 p.
Digital appendices are available in the online Supplements section.

Submitted: August 15, 2022/Accepted: October 7, 2022

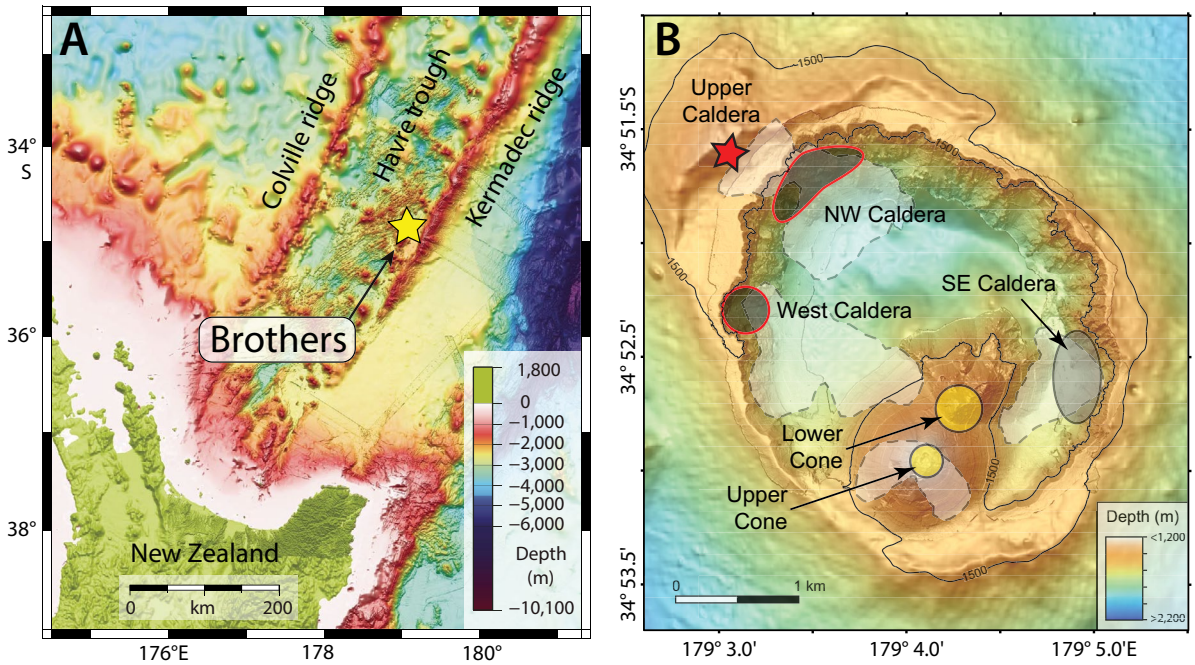

Fig. 1. A) Regional map showing location of Brothers submarine volcano (yellow star) along the active volcanic Kermadec arc north of New Zealand relative to the Kermadec trench, ridge, and backarc features. B) Bathymetry of Brothers with locations of vent fields (dark shaded areas with red borders and red star are high-temperature black smoker vent fields; yellow circles are low-temperature vent fields; the SE Caldera site is currently inactive). Areas of low magnetization (light shaded areas) signify past and present hydrothermal alteration. Black line is the 1,500-m depth contour.

venting at the Lower Cone was similar to hydrothermal venting at the Upper Cone (de Ronde et al., 2011).

A high-resolution, autonomous underwater vehicle (AUV) *ABE* survey in 2007 yielded even more detail on the physical structures within the caldera (Embley et al., 2012). Plume tracers were simultaneously mapped at 50 to 70 m above the sea floor to provide greater resolution of plume type and source locations (Baker et al., 2012). The latter survey led to the discovery of a separate vent field on the western caldera wall (W Caldera site) that was visually confirmed by remotely operated vehicle (ROV) observations during the same expedition, increasing the total number of known vent sites at Brothers to five: the active NW Caldera, W Caldera, Upper Cone, and Lower Cone sites, plus the inactive SE Caldera site. One more active vent field, the Upper Caldera site, was serendipitously discovered during an ROV dive in 2017. While the SE Caldera site is currently inactive (Fig. 1B), that area is characterized by low magnetization and sulfide minerals that indicate high-temperature venting was once present, and was active for a long enough time to significantly alter the magnetic signature of the rocks (Wright et al., 1998; de Ronde et al., 2005; Caratori Tontini et al., 2012).

The progressive discovery of spatially and chemically distinct vent fields at Brothers demonstrates the challenges of comprehensively locating and characterizing separate source locations with a single or short-term survey, especially at a caldera-dominated submarine volcano where plume mixing and accumulation within the caldera can make it more difficult to trace plumes to specific vent fields. Additionally, the numerous studies at Brothers, when combined, describe a dynamic hydrothermal system with measurable changes on scales of years to centuries that has persisted for at least ~1,200 years and most likely a lot longer (de Ronde et al., 2011; Ditchburn et al., 2012; Ditchburn and de Ronde, 2017).

Modeling of Brothers volcano and long-term studies at midocean ridge sites have found connections between plumes in the water column and subseafloor hydrothermal circulation patterns. For example, the Brothers models showed that the different surface expressions of hydrothermal discharge at different locations (i.e., fluids dominated by seawater-rock interactions at the NW Caldera black-smoker vents versus those dominated by magmatic degassing at the Cone sites) can originate from a common deep heat source (Gruen et al., 2012, 2014). These same authors proposed scenarios for how venting and mineral deposition patterns might change as deep hydrothermal circulation evolves after pulses of magmatic fluid perturb the system. Repeat water column surveys at Axial volcano in the northeast Pacific showed that differences in hydrothermal plume enrichments (and subsequent decline) in response to volcanic eruptions could be linked to the distribution of underlying magma chambers (Baker et al., 2019).

In this study, we present a comprehensive compilation of the more than 60 conductivity-temperature-depth (CTD) vertical cast and tow-yo operations completed during the nine hydrothermal plume surveys at Brothers over the span of two decades (1999–2018). This long-term view reveals edifice-wide variability that could not be recognized by any one survey alone. We show that the use of long-term, repeat CTD surveys can be an efficient tool for monitoring the variability of submarine arc hydrothermal systems, which, in turn, can improve understanding of subseafloor circulation, heat and

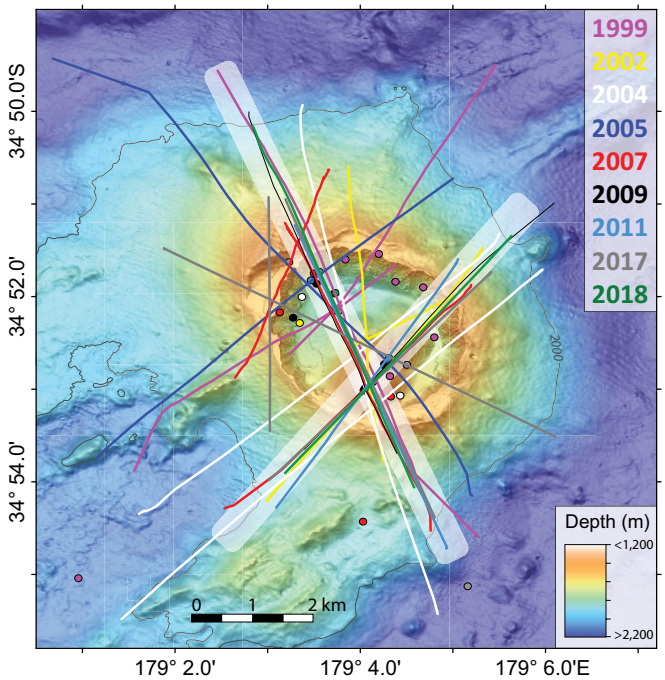

Fig. 2. Station locations for all conductivity-temperature-depth (CTD) tows (lines) and vertical casts (symbols) completed from 1999 to 2018. The two primary tow transects (NW-SE and SW-NE) are highlighted as two bands of light gray.

mass fluxes to the overlying ocean, and the formation of mineral deposits in these environments.

Geologic Setting

The morphology of Brothers volcano (Fig. 1B) is dominated by a ~3- × 3.5-km-wide caldera with a maximum water depth of 1,880 m. Except for a peak on the NW Caldera rim that shoals to ~1,310 m and two resurgent cones that partially merge with the southern caldera wall, a continuous rim depth at ~1,500 m isolates water within the caldera from the surrounding ocean. The rim depth is only slightly deeper (to 1,523 m) in the southwest quadrant, but this depression extends for less than 20% of the caldera rim circumference. The summit depths of the Upper and Lower resurgent cones are ~1,200 and ~1,310 m, respectively. Ring faults within the caldera walls (e.g., Embley et al., 2012) and permeable volcaniclastic deposits composing the cones provide contrasting pathways for hydrothermal circulation and magmatic fluids.

The active vent fields emit fluids with geochemical characteristics that fall into two main categories. The caldera sites (NW Caldera, W Caldera, and Upper Caldera) have high-temperature (to 320°C), acidic (to pH = 3.2), metal-rich fluids characteristic of seawater-rock interactions, and discharge black-smoker plumes through sulfide mineral chimneys. The cone sites (Upper Cone and Lower Cone) emit lower-temperature fluids (typically <120°C, though as high as 200°C for one measurement in 2017) that are more acidic (pH to 1.9), dominated by magmatic gasses (e.g., CO_2, SO_2, H_2S), and occur as diffuse flow, or white smoker (i.e., particulate sulfur) plumes (de Ronde et al., 2005; de Ronde and Stucker, 2015; Kleint et al., 2019; Stucker et al., in press). Deposits on the cones are dominated by native sulfur mounds and iron oxyhydroxide crusts (de Ronde et al., 2011). Vent fluid and hydrothermal deposit compositions at Brothers are well documented elsewhere (de Ronde et al, 2003, 2011; Kleint et al., 2019; Diehl et al., 2020; Stucker et al., in press) and show that the dissolved and particulate chemical compositions of the plumes reflect their different sources (de Ronde et al., 2001; Baker et al., 2003; Massoth et al., 2003).

Fluid inclusions and mineral assemblages within chimneys and hydrothermally altered rocks show that pulses of magmatic gasses, injection of magmatic brines, phase separation, and changes in permeability are some of the subsurface processes that influence vent fluid chemistry and mineralization within the NW Caldera hydrothermal system (de Ronde et al., 2005, 2011, 2019b; Gruen et al., 2014; Diehl et al., 2020; Lee et al., in press). The cone sites are much younger and more magmatically influenced than the NW Caldera site, which suggests a shorter, more direct pathway for magmatic gasses to be discharged at the sea floor (de Ronde et al., 2005, 2019b; Caratori Tontini et al., 2012). Changes in plume chemistry were observed between 1999 and 2002 that indicated a pulse of magmatic gas had been injected into the hydrothermal system during that time interval (de Ronde et al., 2005). Similarly, changes in vent fluid chemistry have identified increased magmatic or seawater-rock influence across all sites on scales of one to 14 years (de Ronde et al., 2011; Stucker et al., in press).

Methods

The nine expeditions that included plume surveys are summarized in Table 1. Hydrothermal plumes were mapped using turbidity and oxidation-reduction potential (ORP) as the primary plume tracers during CTD tows and vertical casts (Fig. 2; App. Fig. A1). Two primary tow transects were repeated each year – one crossing the caldera aligned in a northwest-southeast direction that crossed over the NW Caldera vent field and Upper Cone, the other aligned southwest-northeast to cross over the summits of both the Upper and Lower cones. The direction that each tow was conducted was determined by weather conditions and ship handling requirements at that time (see App. Fig. A1). Most surveys were done over the span of a few days, except for 2018, when the ship occupied the site for 18 days.

The CTD deployed was a Seabird 9*plus* system with integrated optical backscatter (turbidity) and oxidation-reduction potential (ORP) sensors to measure suspended particle concentrations and changes in dissolved chemistry from hydrothermal effluent, respectively: two primary tracers that effectively map dispersing, nonbuoyant hydrothermal plumes. Turbidity is reported as dimensionless nephelometric turbidity units (NTU; American Public Health Association, 1985). The turbidity anomaly (ΔNTU) is the excess value above the local ambient water and is directly correlated with suspended mass concentrations of hydrothermal particles (Baker et al., 2003). However, particle size and composition can affect backscatter efficiency. For example, plumes from high-temperature black smoker systems typically have relatively high suspended mass concentrations. By contrast, sulfur particles found in lower-temperature white-smoker plumes can cause more intense backscatter responses at similar mass concentrations (Baker et al., 2001, 2012). This provides insight into the relative chemistry of the discharging fluids.

Table 1. Summary of Expeditions Between 1999 and 2018 When Hydrothermal Plume Surveys Were Conducted

Mon/Year	Cruise name	Ship	Cruise number	# Tows	# Vertical casts
03/1999	NZAPLUME-I	*R/V Tangaroa*	TAN99-03	3	8
05/2002	NZAPLUME-II	*R/V Tangaroa*	TAN02-06	3	3
10/2004	NZAPLUME-III	*R/V Tangaroa*	TAN04-11	3	3
05/2005	NZASRoF	*R/V Ka'imikai-o-Kanaloa*	KOK-05-05/KOK-05-06	2	1
08/2007	ROVARK	*R/V Sonne*	n.a.	3	5
03/2009	U. Washington	*R/V Thomas G. Thompson*	TN230	2	6
03/2011	NZASMS/OS2020	*R/V Tangaroa*	TAN11-04	2	2
01/2017	Hydrothermadec	*R/V Sonne*	SO253	4	7
03/2018	Brothers Volcano	*R/V Thomas G. Thompson*	TN350	2	2
			Total:	24	37

Note: Individual tow and vertical cast locations for each year are shown in Appendix Figure A1

Plumes from both high- and low-temperature vents contain elevated concentrations of dissolved reduced chemical species (i.e., Fe^{2+}, HS^-, H_2) that are out of equilibrium with the oxidizing ocean. The ORP sensor is a platinum working electrode paired with a silver-silver chloride reference electrode and responds to micromolar concentrations of these reduced hydrothermal chemicals with rapidly decreasing potential (E, mV; Walker et al., 2007; Baker et al., 2016). ORP data was available from 2004 to 2018 (except for 2005). Anomalies are identified by either a time rate of change (dE/dt) greater than the normal drift of the sensor or by the magnitude of the overall drop in potential (ΔE, mV) over the duration of the signal, which qualitatively indicates the intensity of reduced chemical concentrations (Walker et al., 2007).

Miniature autonomous plume recorders (MAPRs; Baker and Milburn, 1997; Walker et al., 2007) attached to AUV and ROV platforms provided additional full water column vertical profiles of the same plume tracers at vehicle descent/ascent locations in 2007, 2011, 2017, and 2018.

Temperature anomalies are less reliably calculated at Brothers due to its location in a hydrographically dynamic region where mesoscale eddies and mixing of water masses regularly affect temperature and salinity distributions within the depth range where plumes disperse (Fig. A2; Roemmich and Sutton, 1998; Stanton, 2002; Lavelle et al., 2008). The resulting nonlinear potential temperature-salinity (θ-S) and potential temperature-potential density (θ-σ_θ) relationships have significant variability over the temporal and spatial scales relevant to our surveys. However, temperature measurements of the sensors we used provide 0.001°C resolution, so relative temperature differences at constant potential density (or depth), or where gradients are low, can effectively identify hydrothermal input. Herein, potential density refers to σ_θ, or the excess relative to 1,000 kg/m^3 referenced to 0 db pressure.

Local currents were directly measured during only three of the plume surveys (2004, 2005, and 2017) and are described in detail elsewhere (Lavelle et al., 2008; Kleint et al., 2022). Lavelle et al. (2008) deployed three moorings with a total of six current meters located to the northeast, southeast, and northwest of the volcano (~7–8 km from the center of the caldera). The current meters were also equipped with temperature sensors and recorded measurements hourly between September 2004 and May 2005. During the 2017 survey, acoustic Doppler current (ADCP) profilers were mounted on the CTD frame (Kleint et al., 2022). Each of these studies also considered potential impacts of the mesoscale eddy field in this region. Water mass properties of the North Cape Eddy, for example, can extend to at least 2,000 m (Sutton and Chereskin, 2002), and anonymously low water temperatures observed as deep as 1,259 m, and possibly deeper, by Lavelle et al. (2008) from December 2004 to March 2005 were related to a cold core eddy positioned just north of Brothers during that time. Rectified oscillatory flow interacting with Brothers topography likely leads to anticyclonic toroidal circulation near the summit, contributing to a generally radial pattern of plume distribution, or "halo," around the edifice, as has been observed at other seamounts (Lavelle et al., 2003; Baker et al., 2004; Staudigel et al., 2004; Lavelle, 2006). Due to these hydrodynamic factors, the hydrothermal plumes originating at Brothers may not consistently stream away from the volcano in a clearly defined direction. Our analyses here focus on rise height and maximum intensity of plume tracer anomalies to look for evidence of changes in the deeper hydrothermal system over time, so while the broader dispersal patterns of the plumes are important for many reasons, they are not essential to this purpose.

Results

General patterns of plume distribution

Plume distributions from the northwest-southeast transects for all years (1999–2018) are shown in Figure 3. Every survey mapped hydrothermal plumes that were distributed in mul-

Fig. 3. Plume distributions for NW-SE transects for each year from 1999 to 2018. The dotted line shows the sawtooth towpath of the conductivity-temperature-depth (CTD); turbidity (ΔNTU) is shown by color-filled contours; the intensity and duration of oxidation-reduction potential (ORP) anomalies (ΔE) are shown as pink to purple colors overlain on the CTD towpath; solid lines are potential density (σ_θ) contours. Color scales are the same for all years. The bathymetry profile along the tow trackline is shown (gray). Thick black line over the bathymetry profile shows the depth range of the NW Caldera vent field. The triangle, dotted line, and solid line positioned over the Upper Cone bathymetry mark the depths of the Upper Cone summit, Lower Cone summit, and Lower Cone reference depth (see text), respectively. The star marks the latitude and depth of the Upper Caldera vent field. Note that the tow trackline in 2005 went over the Upper Caldera peak then passed between the Upper Cone and Lower Cone summits, so a solid line has been added to show the bathymetry profile of the Upper Cone.

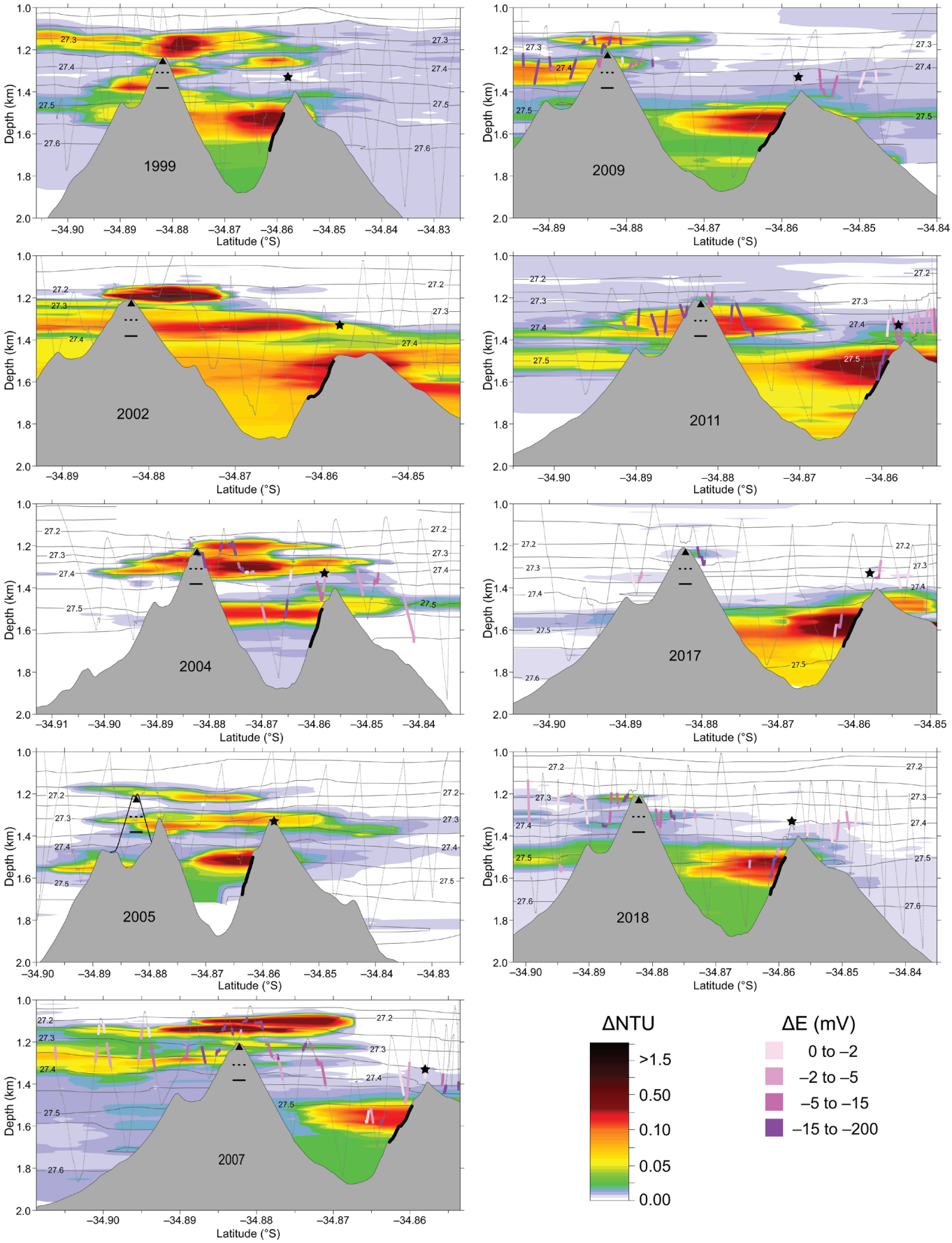

tiple layers between ~1,100 m water depth to the bottom of the caldera (~1,850 m). Several features of plume distributions are common from year to year. Principally, plume depths are correlated with the known depths of the vent fields, and vertical ranges for the horizontally dispersing neutrally buoyant plumes are constrained by isopycnals (i.e., contours of equal density). Plumes from vents located at depths above the caldera rim are immediately subject to dispersal by local and regional currents, while within the caldera, plumes can (1) be wholly or partly trapped, (2) have their upper limits drawn above the rim depth by tidal heave or internal waves to disperse in the surrounding ocean (e.g., Staudigal et al., 2004; Lavelle et al., 2008; Lavelle and Mohn, 2010), and/or (3) be partially or completely removed from the caldera during episodic flushing events.

Plume depths and thicknesses can vary over the time required to complete plume surveys (several hours to days) due to Brothers location in this dynamic hydrographic environment. This is particularly evident in plume distributions between the two primary tow transects, especially where they pass over the cones in any given year (e.g., the Upper Cone plume in Fig. 4; also compare Fig. 3 and App. Fig. A3). However, some plume layers that appear to occur at different depths during different tows (or vertical casts) are actually constrained within the same narrow potential density range, indicating that they are from the same plume source (Figs. 3, 5A-B). Conversely, plumes that appear within the same depth range can actually be dispersing on different isopycnals, which suggests that they originated at different sources.

The variability of potential density at any given depth (i.e., how great the depth difference can be for the same isopycnal) is shown in Figure 5C. In this example, over the span of five days in 2017, the potential density (σ_θ) at the depth of the Upper Cone summit (1,200 m) differed by 0.02, whereas at the caldera rim depth (1,500 m), σ_θ differed by more than 0.08. The depth of the σ_θ = 27.5 isopycnal changed by as much as 130 m. The time and distance between the profiles with the outermost values at 1,500 m was only 2.5 days and 2.5 km, respectively, and both profiles were located on the south-southeast side of Brothers outside the caldera, about 2 km from the rim.

The highly variable background hydrography can have significant consequences when attempting to follow the evolution of vent fluid particulate and dissolved chemistry from specific sources to distal plumes (e.g., Neuholtz et al., 2020; Kleint et al., 2022). While it is unlikely that the depth (and density) difference between plumes from the Upper Cone site (~1,200 m or shallower) can be easily confused with plumes escaping from the caldera (> ~1,450 m), the Upper Caldera site is located at about the same depth as the Lower Cone summit depth (~1,300 m), so plumes from each of these chemically distinct sources can coalesce within the ~1,250- to 1,450-m depth range as they are advected around the summit and dispersed to distal locations. Subtle differences in plume σ_θ and the distribution of ORP anomalies (which will disappear more quickly than particulates) relative to the possible source locations were used to differentiate these plumes.

To evaluate the variability of the hydrothermal system at Brothers over the two decades of this study, we have identified plumes from the four major source sites (Upper Cone, Lower Cone, NW Caldera, and Upper Caldera) based on maximum turbidity anomalies (ΔNTU_{max}), ORP anomalies (ΔE), depth (m), proximity to bathymetric features, and potential density (σ_θ) (Fig. 3; Table 2).

Upper and Lower Cone

The Upper and Lower Cone summits are located at depths of 1,200 and 1,305 m, respectively, well above the ~1,500-m continuous caldera rim. Venting here is characterized by lower-temperature (generally <150°C), magmatically influenced fluids that exit the sea floor as widespread diffuse venting or as more focused white smoker vents (de Ronde et al., 2011; Kleint et al., 2019; Stucker et al., in press). Plumes from these sites disperse directly into a region of the surrounding ocean with relatively strong stratification ($d\sigma_\theta/dz = 7 \times 10^{-4}$ to 1×10^{-3}). Upper Cone plumes occurred at or above the summit of the Upper Cone within the depth range of 1,050 to 1,250 m and ranged in thickness from ~50 to 150 m. Lower Cone plumes were located between ~1,250 and 1,450 m. Lower Cone plume sources include widespread diffuse venting from the summit of the Lower Cone as well as from along the flanks of both the Upper and Lower Cones.

Maximum plume turbidity values for each year (Fig. 6A) were highest in the Upper Cone plumes in 1999, 2002, 2007, and 2009, when ΔNTU_{max} ranged from 1.27 to 2.21, the highest of any of the plumes at Brothers volcano measured during this

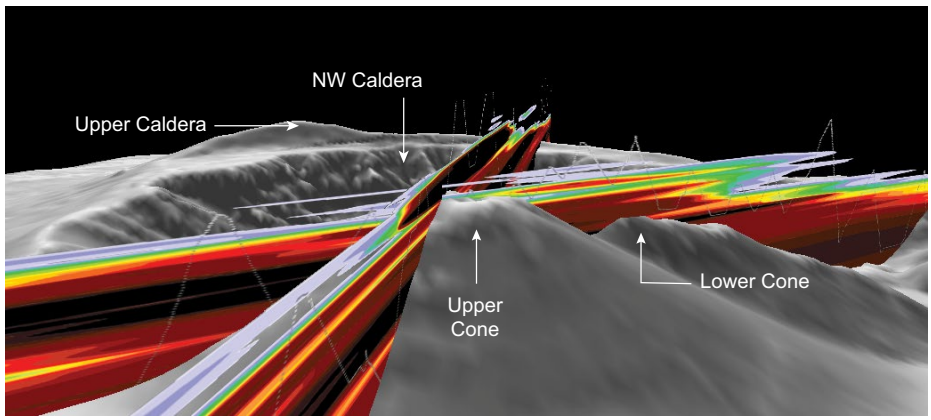

Fig. 4. 3-D view of the difference in rise height, thickness, and turbidity (ΔNTU) intensity for the Upper Cone plume in 2002 from two separate tows (T02A-10 and T02A-12). The time between these two tow sections was about nine hours.

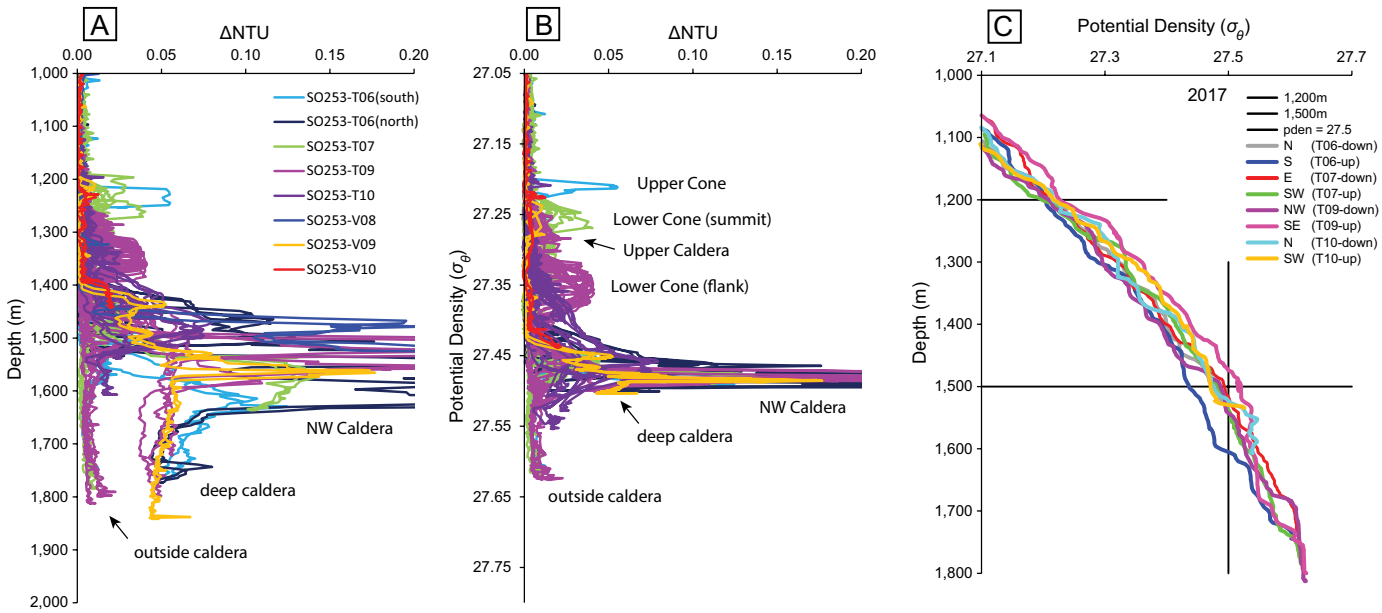

Fig. 5. Profiles of turbidity (ΔNTU) plotted against (A) depth and (B) potential density (σ_θ) for all casts and tows in 2017 showing that, while plume distributions may cover broad depth ranges, the plume maxima are more closely aligned and constrained along isopycnals. C) Potential density plotted against depth. Horizontal lines highlight the range of σ_θ values at the same depth (for Upper Cone summit and continuous caldera rim, 1,200 and 1,500 m, respectively). Vertical line shows range of depth for σ_θ = 27.5 (time and distance between extreme values is discussed in the text).

study, and an order of magnitude more intense than plumes found over midocean ridge (MOR) black smoker vent fields (e.g., Baker et al., 2016). Relatively low values of ΔNTU_{max} (<0.5) were observed in the Upper Cone plume in 2004, 2005, 2011, 2017, and 2018, yet some of these values were still more intense than plumes typically measured along MORs.

Maximum turbidity anomalies in the Lower Cone plumes were generally between ΔNTU_{max} = 0.1 to 0.3, except for a maximum value of ΔNTU_{max} = 0.72 in 2004 when the Lower Cone plume was the most intense from any of the sites, versus a minimum ΔNTU_{max} = 0.04 in 2017. Lower Cone ΔNTU_{max} exceeded Upper Cone values in 2004, 2005, and 2011. The plume from the Lower Cone was distinguishable from the Upper Cone by either a thin layer of reduced turbidity between plume layers, clearly different depths of the ORP anomalies, or both (e.g., 2009 tow transect in Fig. 3). The high ΔNTU values in the Upper and Lower Cone plumes are consistent with hydrothermal particle populations dominated by native sulfur precipitates, as have been characterized for these sites (Massoth et al., 2003; de Ronde et al., 2005; shown in fig. 2D of Stucker et al., in press, as white-yellow "smoke" emanating from vent orifices; see also video at https://www.youtube.com/watch?v=3h-meM8SFZE).

ORP anomalies (ΔE) were colocated with Upper and Lower Cone plume turbidity maximums and had magnitudes of –25 to –100 mV, indicating the presence of significant concentrations of reduced chemical species within these plumes. ORP anomalies diminished in magnitude with distance from the vent sources (Fig. 3), a function of the oxidation rate of the reduced species.

NW Caldera and Upper Caldera

To date, the NW Caldera site is the most robustly defined and studied vent field within the caldera of Brothers volcano.

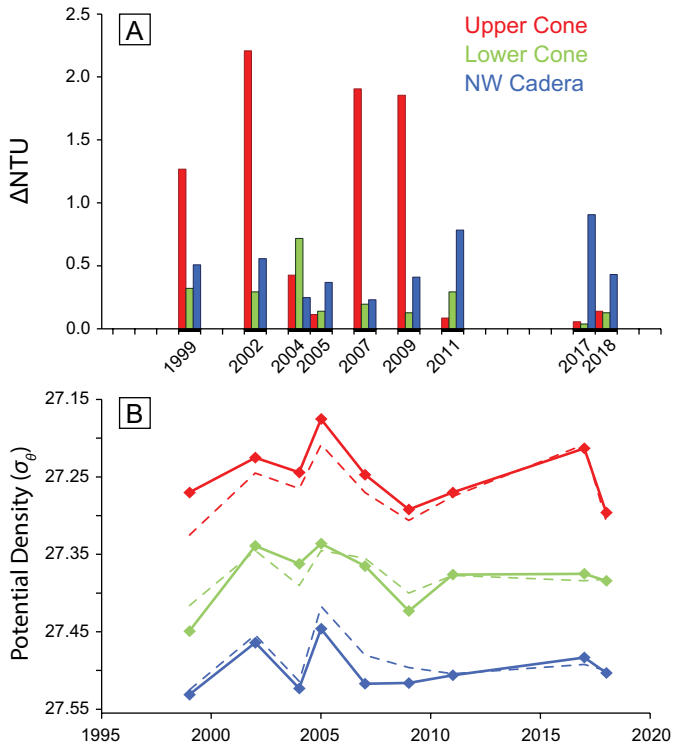

Fig. 6. Relative plume intensity indicators. A) Turbidity (ΔNTU_{max}) for Upper Cone plume (red), Lower Cone plume (green), and NW Caldera plume (blue) for each year surveyed. B) Potential density (σ_θ) of plume ΔNTU_{max} (solid lines with symbols) compared to σ_θ at the reference depth for each plume (dashed lines). Note potential density is plotted with increasing values downward, as it increases with depth. A symbol plotting above the dashed line (i.e., σ_θ at the plume ΔNTU_{max} is less than σ_θ of the reference depth) indicates plume rise above the reference depth. When the symbol plots on or below the dashed line, plume rise is weaker, or sources below the reference depth are dominant. Colors as in A.

Table 2. Summary of Plume Data at ΔNTU_{max} for Upper Cone, Lower Cone, and NW Caldera Plumes for Each Year

Plume Source	Year	ΔNTU_{max}	Depth (m)	ΔE_{max} (mV)	$\sigma_{\theta(\Delta NTU_{max})}$ [1]	$\sigma_{\theta(ref)}$ [2]	$\Delta\sigma_\theta$	$d\sigma_\theta/dz$ [3]
Upper Cone	1999	1.267	1,159	n.d.	27.270	27.325	0.055	7.75E-04
	2002	2.208	1,193	n.d.	27.225	27.245	0.020	7.40E-04
	2004	0.426	1,188	–98	27.244	27.265	0.021	1.08E-03
	2005	0.114	1,218	n.d.	27.175	27.208	0.033	7.80E-04
	2007	1.905	1,139	–109	27.247	27.270	0.023	6.90E-04
	2009	1.854	1,164	–104	27.292	27.306	0.014	6.90E-04
	2011	0.085	1,194	–39	27.270	27.275	0.005	7.30E-04
	2017	0.055	1,239	–69	27.213	27.208	–0.005	1.01E-03
	2018	0.139	1,213	–64	27.296	27.308	0.012	8.30E-04
Lower Cone	1999	0.322	1,381	n.d.	27.449	27.416	–0.033	6.70E-04
	2002	0.293	1,322	n.d.	27.339	27.345	0.006	6.50E-04
	2004	0.718	1,310	–79	27.362	27.390	0.028	1.08E-03
	2005	0.140	1,360	n.d.	27.336	27.345	0.009	6.90E-04
	2007	0.195	1,282	–29	27.365	27.355	–0.010	6.90E-04
	2009	0.127	1,344	–239	27.423	27.400	–0.023	6.90E-04
	2011	0.294	1,310	–174	27.376	27.377	0.001	7.30E-04
	2017	0.039	1,344	–99	27.375	27.384	0.009	8.70E-04
	2018	0.128	1,307	–62	27.384	27.382	–0.002	8.30E-04
NW Caldera	1999	0.509	1,532	n.d.	27.531	27.525	–0.006	4.20E-04
	2002	0.557	1,569	n.d.	27.464	27.454	–0.010	3.80E-04
	2004	0.248	1,518	–27	27.523	27.514	–0.009	4.70E-04
	2005	0.369	1,509	n.d.	27.446	27.417	–0.029	6.00E-04
	2007	0.231	1,531	–43	27.517	27.480	–0.037	6.90E-04
	2009	0.410	1,556	–73	27.516	27.496	–0.020	3.90E-04
	2011	0.784	1,490	–106	27.506	27.504	–0.002	4.90E-04
	2017	0.907	1,548	–67	27.483	27.492	0.009	5.30E-04
	2018	0.431	1,522	–77	27.503	27.500	–0.003	4.70E-04
Deep caldera	1999	0.022	1,829	n.a	27.5435	n.a.	n.a.	5.00E-05
	2002	0.044	1,852		27.4748			4.30E-05
	2004	0.014	1,822		27.5366			5.90E-05
	2005	0.020	1,630		27.4621			7.80E-05
	2007	0.020	1,830		27.5318			7.20E-05
	2009	0.023	1,794		27.5290			8.60E-05
	2011	0.031	1,781		27.5244			6.90E-05
	2017	0.044	1,833		27.5031			5.00E-05
	2018	0.030	1,823		27.5184			5.90E-05

NOTES: n.d. = no data; n.a. = not applicable; the Upper Caldera plume is not included in this table because the source location was not known until 2017, thus conductivity-temperature-depth (CTD) locations were not optimal for sampling plume maxima in prior years

[1]Potential density at the plume ΔNTU_{max}

[2]Potential density at the reference depth for each plume (Upper Cone = 1,200 m; Lower Cone = 1,380 m; NW Caldera = 1,500 m)

[3]Density gradient ($d\sigma_\theta/dz$) was calculated for an appropriate depth range for each plume level in each year

The standard NW-SE tow was designed to sample over this site, across the caldera, and over (or between) the cone summits. We acknowledge that the plume referred to here as the NW Caldera plume is actually the product of all hydrothermal sources within the caldera deeper than ~1,540 m, including the known West Caldera vents. However, comprehensive, high-resolution plume mapping within the caldera using *ABE* showed the NW Caldera site is the largest and most vigorous vent field (Baker et al., 2012) and dominantly contributes to the NW Caldera plume. Turbidity and ΔE distributions presented here also support the NW Caldera site as the dominant contributor to within-caldera hydrothermal products.

In all years, plumes surrounding the volcano outside the caldera at rim depth, or slightly deeper, are evidence that some hydrothermal products routinely escape from the caldera. This has previously been attributed to tidal pumping by Baker et al. (2003). However, additional contributions likely come from diffuse venting that occurs along the caldera rim platform, vents located on or near the top of the caldera wall where plumes might rise above the caldera rim, and/or episodic whole-caldera flushing events that are evident in the 20-year perspective presented here.

NW Caldera plume turbidity ranged from ΔNTU_{max} = 0.23 to 0.91, with minimum and maximum values occurring in 2007 and 2017, respectively (Fig. 6A). Outside the caldera, the upper boundary of the plume was always deeper than ~1,430 m, with plume ΔNTU_{max} at σ_θ = 27.5 ± 0.03. Within the caldera, the bottom of the ΔNTU_{max} layer extended to ~1,650 m. Additionally, hydrothermal particulates were trapped within the deepest parts of the caldera to varying degrees (ΔNTU = 0.014–0.044, comparable to values seen at many MOR vent fields) during each of our plume surveys (Fig. 3; Table 2). The NW Caldera plumes were the most intense plumes at Brothers volcano in 2011, 2017, and 2018, when the Upper Cone plume was at a minimum.

ORP anomalies in the NW Caldera plume were generally less intense (ΔE = –10 to –20 mV) than the anomalies associated with the Upper and Lower Cone plumes, unless the

CTD passed close to the NW Caldera vent field (e.g., ΔE = –70 to –100 mV in 2017 and 2018; Fig. 3). ORP anomalies were also observed above and outside the caldera rim to the north at depths as shallow as ~1,300 m, and in retrospect, were indications that the (up until that point undiscovered) Upper Caldera site was active throughout the study period. A high-resolution bathymetric survey conducted with the ROV *Jason* in 2018 mapped the shallow peak of the caldera rim where the Upper Caldera site is located, revealing a 120- × 70-m chimney field at a depth of 1,325 to 1,345 m and two smaller chimney fields (one ~80 × 100 m at 1,374–1,406 m depth on the south side of the rim, and the other about 40 × 20 m at 1,400 m on the north side of the rim; de Ronde et al., in press). MAPR instruments attached to *Jason* mapped turbidity and ORP anomalies in the water column near each of these chimney fields, and the northwest-southeast CTD tow transects in nearly all years showed anomalies on the north side of the rim that were, at the time, interpreted as being related to the NW Caldera plume spilling over the north rim of the caldera. However, it appears from the plume survey data that, while some portion of this suspended particle population likely originates from the NW Caldera vent field, the ORP anomalies mapped during the ROV *Jason* high-resolution bathymetric surveys (conducted with the ROV at 30 and 70 m above the sea floor) strongly suggest that all these chimney clusters are also active. Additional direct sea-floor observations will be necessary to fully map and characterize all active vents within these chimney clusters, and to assess how far activity may extend along the outer north flank.

Discussion

Rise height as an indicator of hydrothermal system intensity

Plume distributions at Brothers clearly show differences in optical intensity and vertical distribution over time, which suggest significant source flux variability. The rise height of a nonbuoyant plume is related to the heat and mass flux from a vent field (McDougall, 1990; Lupton, 1995; Baker et al., 2019), but using depth intervals to determine rise height can be misleading due to complicating factors such as changes in ambient water column stratification (Fig. 5C), tidal oscillations, and plume blow-down by cross-flow currents (Lavelle, 1997; Xu and Lavelle, 2017; Baker et al., 2019). Instead, the difference between σ_θ at plume ΔNTU_{max} compared to σ_θ at a reference depth ($\Delta\sigma_\theta$) for each major plume level over time (Fig. 6B) was used as a proxy for rise height, hence heat flux, to minimize the effects of these confounding factors (Baker et al., 2019). The reference depths selected were 1,200 m for the Upper Cone plume, 1,380 m for the Lower Cone plume, and 1,500 m (the continuous caldera rim depth) for the NW Caldera plume. These levels were chosen for the following reasons:

1. 1,200 m is the shallowest depth of the Upper Cone, and vent sources are known to occur within ~30 m of the summit, so $\Delta\sigma_\theta$ for the Upper Cone plumes are minimum values and relative changes likely reflect actual changes in heat and volume flux from the Upper Cone vent field.
2. Sources that contribute to the Lower Cone plume are more widespread (i.e., located along the flanks of both the Upper and Lower Cones as well as at the summit of the Lower Cone), and sea-floor exploration of the flanks deeper than ~1,350 is incomplete, thus there may be additional sources deeper along the flanks of the Lower Cone. Comparing σ_θ of the Lower Cone ΔNTU_{max} to that of the reference depth can be used to infer the depth range where most intense discharge from this area may be occurring (i.e., above or below the reference depth);
3. The continuous caldera rim depth (1,500 m) was selected as the reference depth for the NW Caldera plume because stratification above the caldera rim is an order of magnitude greater than within the caldera (Table 2), which limits the vertical extent of the NW Caldera plume (Fig. 3). Within the caldera, where stratification is weak, plumes from the vent field can easily rise from the deepest active chimneys at ~1,700 m to near the rim depth, but further vertical rise of the plume is hindered by increased stratification above the caldera rim. If NW Caldera plume σ_θ is equal to, or less than, the reference depth σ_θ, there is a greater likelihood for hydrothermal products from within the caldera to be dispersed to the ocean outside the caldera.

From 1999 to 2009, the Upper Cone plume had exceptionally high turbidity anomalies (ΔNTU_{max} = 1.27–2.21, except for 2004) with plume rise heights up to $\Delta\sigma_\theta$ = 0.055. Both of these measures of plume intensity were significantly diminished in 2011 to 2018, when rise height was negligible and turbidity had decreased by an order of magnitude, suggesting greatly reduced hydrothermal flux from the Brothers Upper Cone during that time.

Conversely, from 2011 to 2018, the NW Caldera plume replaced the Upper Cone as the dominant source of hydrothermal particulates at Brothers, and $\Delta\sigma_\theta$ was near zero, or slightly positive (meaning the plume rose to, or above, the reference depth), an indication of increased rise height and hydrothermal output from the NW Caldera vent field. Despite a gap of six years between the 2011 and 2017 surveys, hydrothermal output appears to have increased within the caldera sometime after the 2009 survey while simultaneously decreasing in intensity at the Upper Cone site.

The Lower Cone plume ΔNTU_{max} occurred at, or above, the reference depth (σ_θ) in all years except 1999, 2007, and 2009, which suggests hydrothermal output was dominant on the flanks of the Upper Cone and/or summit of the Lower Cone for most years, but was invigorated at deeper sources in 1999, 2007, and 2009. Modeling by Gruen et al. (2014) predicted that lateral flow of magmatic brines within the porous sea floor composing the cones could increase as the hydrothermal system evolved following a pulse of magmatic fluids and could thus result in increased venting deeper on the flanks of the cones. Iron oxide crusts found on the Upper Cone flank that were determined to have been deposited sometime between 1999 and 2002 by fluids that ponded around boulders or flowed downslope (de Ronde et al., 2011) demonstrate that fluids with negative buoyancy can occur. However, the nonbuoyant plume data cannot resolve the difference between plumes found deeper than the Lower Cone reference depth as being generated from negatively buoyant fluids or newly-invigorated deeper sources.

Taken together, these observations show that long-term plume distribution surveys can be a useful tool for identifying

edifice-scale shifts in hydrothermal circulation patterns on the scale of years to decades. This in turn may ultimately reflect subtle changes in mineralization below the sea floor, contribute to mineral assemblage zonation in sulfide chimneys, and potentially provide insight from a modern system for workers looking at mineralization of ancient systems. For example, de Ronde et al. (2011) found two dominant types of sulfide mineralization in NW Caldera vent field deposits: Cu-rich and Zn-rich. Interlayered zones of the different mineral types recorded periods of high-temperature fluid flow (Cu-rich minerals) with zones formed during periods of relatively cooler flow (Zn-rich minerals). The layers were correlated with age, indicating that variable physiochemical conditions influenced the character of mineral deposition at different times over the lifetime of a four-year-old chimney.

Caldera flushing events

Water within the deepest part of the caldera is isolated from the surrounding ocean and has the same temperature, salinity, and density properties of the water located close to the caldera rim depth (Fig. A4). The density gradient within the caldera ($6.3 \times 10^{-5} \pm 1.4 \times 10^{-5}$) is an order of magnitude weaker than the water column at the caldera rim depth ($4.9 \times 10^{-4} \pm 1.0 \times 10^{-4}$; Table 2). Turbidity within the deep caldera (i.e., below the NW Caldera plume turbidity maxima) varied from a high $\Delta NTU_{max} = 0.044$ in 2002 and 2017 to a minimum $\Delta NTU_{max} = 0.014$ in 2004. While deep caldera turbidity was positively correlated with NW Caldera plume ΔNTU_{max} ($r^2 = 0.6$; Fig. A5), it was an order of magnitude lower. The most likely sources for the deep caldera particles are (1) particles settling directly out of the NW Caldera plume, (2) ongoing precipitation/oxidation of dissolved constituents, then settling or recirculating, from the NW Caldera plume, and/or (3) resuspension of sediments within the caldera. It is also possible a vertical circulation cell has been established within the weakly stratified body of water filling the caldera (German and Sparks, 1993; Hart et al., 2003). Driven by buoyant plumes from chimneys along the caldera walls and capped by the steeper density gradient at the caldera rim, a fraction of the NW Caldera plume could be drawn deeper into the caldera to replace the water rising at the chimneys, thereby recirculating and distributing particulates to deeper depths throughout the caldera.

Water from outside the caldera can displace water within the caldera (along with its particulate and dissolved components) only when an external water mass with greater density than the deep caldera contents moves across the caldera rim. Staudigel et al. (2004) were able to monitor infiltration of external seawater into the caldera at Vailulu'u, the youngest volcano in the Samoan chain and current location of the Samoan hotspot, using moored temperature sensors placed at caldera rim breaches and the bottom of the caldera. Temperature variations occurred at tidal frequencies and were related to 50- to 100-m vertical displacement of isotherms, allowing for near-continuous additions of external water to the caldera and ventilation of hydrothermal products to the surrounding ocean. However, one major difference between Vailulu'u and Brothers is that the continuous caldera rim depth at Vailulu'u is much shallower (~800 m) than the rim at Brothers and is in a region of the water column where there are steeper temperature gradients. A similar process related to tidal energy is likely for Brothers (Lavelle and Mohn, 2010), but temperature (and density) differences with tidal heave will be smaller at the Brothers caldera rim depths, with a correspondingly smaller effect.

Another process that could be responsible for partial or full caldera flushing events at Brothers is the passage of mesoscale eddies over the caldera. These are well documented to occur in the region where Brothers volcano is located north of New Zealand, are highly variable, and can impact water mass properties to depths >2,000 m (Roemmich and Sutton, 1998; Sutton and Chereskin, 2002). Lavelle et al. (2008) documented a cold water mass passing over Brothers from December 2004 through February 2005 that was detected in all moored sensors (to 1,600 m). There was no corresponding data to confirm how that may have affected water within the caldera during that time, but it demonstrates the possibility of a cold core eddy of sufficient size and duration to impact Brothers caldera.

Our plume surveys are "snapshots" in time, and do not provide any information on the actual frequency, time required for flushing events to replace the water within the caldera, or the period of time for the deep caldera to remain isolated long enough to accumulate the concentrations of suspended particulates observed after full or partial removal. The cold core eddy seen by Lavelle et al. (2008) was present over Brothers volcano for three months, and the intervals between our surveys ranged from seven months to 5.8 years with differences seen between all surveys, so this process must occur repeatedly and on the scale of months to years. The suspended particles subject to this mode of dispersal (or accumulation) are predominantly from the metal-rich, high-temperature vents within the caldera, thus will lead to deposition of metal-rich sediments to both the caldera floor and the surrounding region.

The caldera as a calorimeter

The majority of our plume surveys at Brothers volcano were completed within two to three days, but in 2018, while on site for 18 days, a series of vertical CTD casts were repeated at the same location in the deepest part of the caldera. These casts showed a progressive increase in temperature deeper than 1,570 m (Fig. 7), i.e., below the level where inside/outside water properties bifurcated in 2018. The water outside the caldera at caldera rim depth was not denser than the water within the deep caldera, indicating that the contents of the caldera were well isolated and not being infiltrated by outside water during this time. Therefore, the temperature increase below 1,570 m can be interpreted as the net conductive plus advective heat flux below this depth.

Heat flux studies using thermal blankets (Caratori Tontini et al., 2012) found very low or negative conductive heat flux across the caldera floor, indicating this area serves as a recharge zone for the Brothers hydrothermal system. It is likely that the majority of heat contributing to the observed temperature increase comes from diffuse and/or focused venting along the caldera walls deeper than 1,570 m (σ_θ = 27.51 in 2018), i.e., the sources indicated by plume anomalies mapped at 1,650- to 1,750-m depths along the caldera walls by Baker et al. (2012). Using the volume of the caldera below

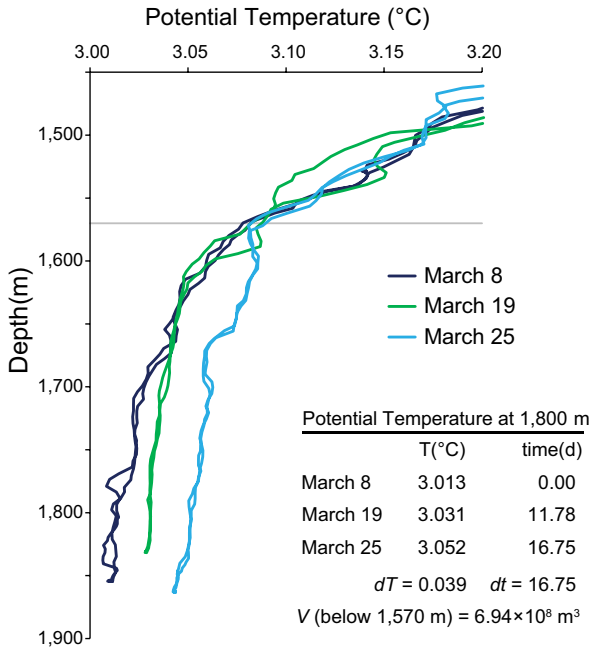

Fig. 7. Potential temperature profiles inside the deep caldera showing progressive increase over 17 days in March 2018. Inset table shows the values used to calculate heat flux (see text). The 1,570-m depth, below which water within the caldera is isolated from the surrounding ocean in 2018, is marked by the gray line.

this depth as a calorimeter, the heat flux to this body of water can be calculated using the following equation:

$$E = \rho V C_p (dT/dt) \quad (1)$$

where ρ is the density of seawater in the deep caldera (1,027.5 kg/m^3), V is the volume of the caldera below 1,570 m (6.94×10^8 m^3), C_p is the specific heat capacity for seawater (3,985 J/kg°C), and the change in temperature over time = dT/dt = 0.039°C/16.75 days, resulting in a heat flux of ~79 MW.

This is a minimum value for the deep caldera only, not for Brothers volcano as a whole. Heat flux from the Upper and Lower Cone and Upper Caldera plumes is discharged directly to the ocean at much shallower depths, and a significant portion of NW Caldera plume (typically centered at σ_θ ~27.5) was also located above the fully isolated caldera depth, but still mostly below the caldera rim (the depth of bifurcation in temperature, salinity, and density profiles ranged from 1,530–1,570 m during our surveys). However, identifying even a small portion of the total heat flux can add to our understanding of the hydrothermal system overall and serve as a baseline for comparison with other sites and future studies at Brothers. For example, using a different method, Staudigel et al. (2004) estimated heat flux an order of magnitude greater (760 MW) from the Vailulu'u caldera, but nearly all the hydrothermal discharge there was located well below the caldera rim at that time.

We also note that turbidity did not follow the same increasing trend as temperature, indicating that processes controlling the distribution of heat and particles are decoupled. For example, there are no conductive sources for particles throughout the caldera, and oxidation or settling rates will not impact heat distribution.

Summary and Conclusion

Brothers submarine arc volcano hosts a robust hydrothermal system with variable surface expressions at multiple sites across the edifice. Hydrothermal plumes emanating from these sites have distinct patterns of distribution such that plumes can be differentiated and related to their sources generally by depth, but more accurately by the density level of their neutrally buoyant plumes. While hydrothermal temperature anomalies are largely obscured by the variability in regional hydrographic properties (e.g., potential temperature, salinity, and potential density) at distance and time scales of plume mapping surveys, plume intensity (in this case, measured by turbidity and rise height expressed as $\Delta\sigma_\theta$ compared to a reference depth) can be used to infer invigoration (or decline) of hydrothermal output from the different vent fields. Changes in plume intensity between 1999 and 2018 suggested that hydrothermal output changed inversely between the cone and caldera sites sometime between 2009 and 2011, with greater hydrothermal output shifting from the magmatic fluid-influenced cones to the seawater-rock–dominated caldera. This apparently coordinated shift supports interpretations based on other evidence (e.g., vent fluid chemistry) that all venting at Brothers is linked to a deeper, shared hydrothermal circulation system. The model of Gruen et al. (2014) estimated that deep hydrothermal system changes that could impact the location and assemblage of mineral deposits occurred over hundreds of years. However, ages and mineral zonation within chimneys (de Ronde et al., 2011; Berkenbosch et al., 2012, 2019), changes in vent fluid chemistry (Stucker et al., in press, and references therein), and this plume study indicate that time scales can also be on the order of years to decades.

In addition to the Brothers hydrothermal system being an important analog for the formation of mineral deposits, the Brothers caldera volcano can be a valuable natural laboratory for investigating plume dissolved and particulate chemical evolution from high-temperature black smoker vent fields during periods when hydrothermal products are trapped within the caldera. More information is needed to determine the time scales over which the deep caldera (1) remains isolated from the surrounding ocean, and (2) is infiltrated in whole, or in part, to disperse hydrothermal products more broadly in the region. The measurable and progressive temperature increase over the span of ~17 days demonstrates the potential for such studies. The heat flux calculated from those data are an order of magnitude lower (79 MW) than was estimated for Vailulu'u (760 MW), but unlike Vailulu'u where all known hydrothermal discharge was located near the bottom of the caldera at the time, there is copious venting at Brothers discharging well above the caldera rim, which would not be include in the calculation.

Brothers is also an interesting site for studying the influence of regional mesoscale eddies on the hydrothermal system and any role they may have in dispersing hydrothermal heat and mass throughout the region. Dispersal of a variable fraction of heat and mass from the caldera likely occurs on a continuous basis due to regular tidal heave, but the intermittent "snapshot" nature of our surveys is not adequate for systematically determining the frequency of episodic caldera flush-

ing events, the completeness of caldera water mass removal, or the dominant processes that drive those events. Presumably, the removal of hydrothermal heat and chemicals from the caldera occurs across a continuum between no removal and complete removal, with intermediate amounts of transfer possible at any point between the extremes. Frequent CTD-based hydrothermal plume surveys and/or moorings utilizing arrays of similar sensors are cost-effective tools for investigating these questions.

Finally, our time-series plume study shows that active sea-floor hydrothermal systems like those at Brothers provide insight into episodic fluctuations in hydrothermal activity and the preponderance of one type of mineralizing fluid over another to circulate through and/or be discharged from submarine arc volcanoes. In addition to being an efficient exploration tool for the prospecting of modern sea-floor mineralized systems, hydrothermal plume studies can also provide a modern lens through which to view the distribution of metals seen in ancient massive sulfide deposits formed at, or near, the sea floor.

Acknowledgments

The authors wish to thank all the captains, crew, and science party participants who contributed to the successful completion of these plume surveys. Special thanks and appreciation go to Edward T. Baker for his enduring vision, skill, and support through his role as scientist, colleague, friend, and mentor. We thank Jonguk Kim and an anonymous reviewer for their helpful comments that improved the manuscript. CdR would like to acknowledge the Strategic Science Investment Fund (SSIF) at GNS for funding. This is PMEL contribution number 5400.

REFERENCES

American Public Health Association (APHA), 1985, Standard methods for the examination of water and wastewater, 16th ed.: APHA, AWWA, and WPCF joint publication, Washington, DC, 1268 p.

Baker, E.T., and Milburn, H.B., 1997, MAPR: A new instrument for hydrothermal plume mapping: RIDGE Events, v. 8, p. 23–25.

Baker, E.T., Tennant, D.A., Feely, R.A., Lebon, G.T., and Walker, S.L., 2001, Field and laboratory studies on the effect of particle size and composition on optical backscattering measurements in hydrothermal plumes: Deep Sea Research I, v. 48, p. 593–604.

Baker, E.T., Feely, R.A., de Ronde, C.E.J., Massoth, G.J., and Wright, I.C., 2003, Submarine hydrothermal venting on the southern Kermadec volcanic arc front (offshore New Zealand): Location and extent of particle plume signatures: Geological Society of London, Special Publication 219, p. 141–161.

Baker, E.T., Lowell, R.P., Resing, J.A., Feely, R.A., Embley, R.W., Massoth, G.J., and Walker, S.L., 2004, Decay of hydrothermal output following the 1998 seafloor eruption at Axial Volcano: Observations and models: Journal of Geophysical Research, v. 109, B01205, doi: 10.1029/2003JB002618.

Baker, E.T., Walker, S.L., Embley, R.W., and de Ronde, C.E.J., 2012, High-resolution hydrothermal mapping of Brothers Caldera, Kermadec arc: Economic Geology, v. 107, p. 1583–1593, doi: 10.2113/econgeo.107.8.1583.

Baker, E.T., Resing, J.A., Haymon, R.M., Tunnicliffe, V., Lavelle, J.W., Martinez, F., Ferrini, V., Walker, S.L., and Nakamura, K., 2016, How many vent fields? New estimates of vent field populations on ocean ridges from precise mapping of hydrothermal discharge locations: Earth and Planetary Science Letters, v. 449, p. 186–196, doi: 10.1016/j.epsl.2016.05.031.

Baker, E.T., Walker, S.L., Chadwick, W.W., Jr., Butterfield, D.A., Buck, N.J., and Resing, J.A., 2019, Posteruption enhancement of hydrothermal activity: A 33-year, multieruption time series at Axial Seamount (Juan de Fuca Ridge): Geochemistry, Geophysics, Geosystems, v. 20, p. 814–828, doi: 10.1029/2018GC007802.

Berkenbosch, H.A., de Ronde, C.E.J., Gemmell, J.B., McNeill, A.W., and Goemann, K., 2012, Mineralogy and formation of black smoker chimneys from Brothers submarine volcano, Kermadec arc: Economic Geology, v. 107, p. 1613–1633, doi:10.2113/econgeo.107.8.1613.

Berkenbosch, H.A., de Ronde, C.E.J., Ryan, C.G., McNeill, A.W., Howard, D.L., Gemmell, J.B., and Danyushevsky, L.V., 2019, Trace element mapping of copper- and zinc-rich black smoker chimneys from Brothers volcano, Kermadec arc, using synchrotron radiation XFM and LA-ICP-MS: Economic Geology, v. 114, p. 67–92, doi:10.5382/econgeo.2019.4620.

Caratori Tontini, F., Davy, B., de Ronde, C.E.J., Embley, R.W., Leybourne, M., and Tivey, M.A., 2012, Crustal magnetization of Brothers volcano, New Zealand, measured by autonomous underwater vehicles: Geophysical expression of a submarine hydrothermal system: Economic Geology, v. 107, p. 1571–1581, doi: 10.2113/econgeo.107.8.1583.

Caratori Tontini, F., Tivey, M.A., de Ronde, C.E.J., and Humphris, S.E., 2019, Heat flow and near-seafloor magnetic anomalies highlight hydrothermal circulation at Brothers volcano caldera, Southern Kermade arc, New Zealand: Geophysical Research Letters, v. 46, p. 8252–8260, doi: 10.1029/2019GL083517.

Clark, M.R., and O'Shea, S., 2001, Hydrothermal vent and seamount fauna from the southern Kermadec Ridge, New Zealand: InterRidge News, 10b.

de Ronde, C.E.J., Baker, E.T., Massoth, G.J., Lupton, J.E., Wright, I.C., Feely, R.A., and Greene, R.R., 2001, Intra-oceanic subduction-related hydrothermal venting, Kermadec volcanic arc, New Zealand: Earth and Planetary Science Letters, v. 193(3–4), p. 359–369, doi: 10.1016/S0012-821X(01)00534-9.

de Ronde, C.E.J., Faure, K., Bray, C.J., Chappell, D.A., and Wright, I.C., 2003, Hydrothermal fluids associated with seafloor mineralization at two southern Kermadec arc volcanoes, offshore New Zealand: Mineralium Deposita, v. 38, p. 217–233, doi: 10.1007/s00126-002-0305-4.

de Ronde, C.E.J., Hannington, M.D., Stoffers, P., Wright, I.C., Ditchburn, R.G., Reyes, A.G., Baker, E.T., Massoth, G.J., Lupton, J.E., Walker, S.L., Greene, R.R., Soong, C.W.R., Ishibashi, J., Lebon, G.T., Bray, C.J., and Resing, J.A., 2005, Evolution of a submarine magmatic-hydrothermal system: Brothers volcano, southern Kermadec arc, New Zealand: Economic Geology, v. 100, p. 1097–1133, doi: 10.2113/gsecongeo.100.6.1097.

de Ronde, C.E.J., Massoth, G.J., Butterfield, D.A., Christenson, B.W., Ishibashi, J., Ditchburn, R.G., Hannington, M.D., Brathwaite, R.L., Lupton, J.E., Kamenetsky, V.S., Graham, I.J., Zellmer, G.F., Dziak, R.P., Embley, R.W., Dekov, V.M., Munnik, F., Lahr, J., Evans, L.J., and Takai, K., 2011, Submarine hydrothermal activity and gold-rich mineralization at Brothers volcano, Kermadec arc, New Zealand: Mineralium Deposita, v. 46, p. 541–584, doi:10.1007/s00126-011-0345-8.

de Ronde, C.E.J., and Stucker, V.K., 2015, Seafloor hydrothermal venting at volcanic arcs and backarcs, *in* Sigurdsson, H., ed., The encyclopedia of volcanoes, 2nd ed: Academic Press, doi: 10.1016/B978-0-12-385938-9.00047-X.

de Ronde, C.E.J., Humphris, S.E., Höfig, T.W., and the Expedition 376 Scientists, 2019a, Proceedings of the International Ocean Discovery Program, v. 376, doi: 10.14379/iodp.proc.376.101.2019, http://publications.iodp.org/proceedings/376/376title.html.

de Ronde, C.E.J., Humphris, S.E., Höfig, T.W., Reyes, A.G., and the Expedition 376 Scientists, 2019b, Critical role of caldera collapse in the formation of seafloor mineralization: The case of Brothers volcano: Geology, v. 47, p. 762–766, doi: 10.1130/G46047.1.

de Ronde, C.E.J., Humphris, S.E., and Höfig, T.W., in press, IODP Expedition 376 to Brothers volcano: Insights into the inner workings of a subsea-floor hydrothermal system—Introduction: Economic Geology.

Diehl, A., de Ronde, C.E.J., and Bach, W., 2020, Fluid inclusions in hydrothermal precipitates from the NW Caldera hydrothermal vent field, Brothers volcano: Evidence for subcritical phase-separation and occurrence of deep-seated brines: Geofluids, 2020, Article ID 8868259, doi: 10.1155/2020/8868259.

Ditchburn, R.G., de Ronde, C.E.J., and Barry, B.J., 2012, Radiometric dating of volcanic massive sulfides and associated iron oxide crusts with an emphasis on $^{226}Ra/Ba$ and $^{228}Ra/^{226}Ra$ in volcanic and hydrothermal processes at intraoceanic arcs: Economic Geology, v. 107, p. 1635–1648, doi: 10.2113/econgeo.107.8.1635 .

Ditchburn, R.G., and de Ronde, C.E.J., 2017, Evidence for remobilization of barite affecting radiometric dating using ^{228}Ra, ^{228}Th and $^{226}Ra/Ba$ values: Implications for the evolution of seafloor volcanogenic massive: Economic Geology, v. 112, p. 1231–1245, doi: 10.5382/econgeo.2017.4508.

Dziak, R.P., Haxel, J.H., Matsumoto, H., Lau, T.K., Merle, S.G., de Ronde, C.E.J., Embley, R.W., and Mellinger, D.K., 2008, Observations of regional seismicity and local harmonic tremor at Brothers volcano, south Kermadec

arc, using an ocean bottom hydrophone array: Journal of Geophysical Research, v. 113, B09S04, doi: 10.1029/2007JB005533.

Embley, R.W., deRonde, C.E.J., Merle, S.G., Davy, B., and Caratori Tontini, F., 2012, Detailed morphology and structure of an active submarine arc caldera: Brothers volcano, Kermadec arc: Economic Geology, v. 107, p. 1557–1570, doi: 10.2113/econgeo.107.8.1557.

German, C.R., and Sparks, R.S.J., 1993, Particle recycling in the TAG hydrothermal plume: Earth and Planetary Science Letters, v. 116, p. 129–134.

Gruen, G., Weis, P., Driesner, T., de Ronde, C.E.J., and Heinrich, C.A., 2012, Fluid-flow patterns at Brothers volcano, southern Kermadec arc: Insights from geologically constrained numerical simulations: Economic Geology, v. 107, p. 1595–1611.

Gruen, G., Weis, P., Driesner, T., Heinrich, C.A., and de Ronde, C.E.J., 2014, Hydrodynamic modeling of magmatic-hydrothermal activity at submarine arc volcanoes, with implications for ore formation: Earth and Planetary Science Letters, v. 404, p. 307–318.

Hart, S.R., Staudigel, H., Workman, R., Koppers, A.A.P., and Girard, A.P., 2003, A flourescein tracer release experiment in the hydrothermally active crater of Vailulu'u volcano, Samoa: Journal of Geophysical Research, v. 108, B8, 2377, doi:10.1029/2002JB001902.

Kleint, C., Bach, W., Diehl, A., Fröhberg, N., Garbe-Schönberg, D., Hartman, J.F., de Ronde, C.E.J., Sander, S.G., Strauss, H., Stucker, V.K., Thal, J., Zitoun, R., and Koschinsky, A., 2019, Geochemical characterization of highly diverse hydrothermal fluids from volcanic vent systems of the Kermadec intraoceanic arc: Chemical Geology, v. 528, article 119289, doi: 10.1016/j.chemgeo.2019.119289.

Kleint, C., Zitoun, R., Neuholz, R., Walter, M., Schnetger, B., Klose, L., Chiswell, S.M., Middag, R., Laan, P., Sander, S.G., and Koschinsky, A., 2022, Trace metal dynamics in shallow hydrothermal plumes at the Kermadec arc: Frontiers in Marine Science, v. 8, article 782734, doi: 10.3389/fmars.2021.782734.

Lavelle, J.W., 1997, Buoyancy-driven plumes in rotating, stratified cross flows: Plume dependence on rotation, turbulent mixing, and cross-flow strength: Journal of Geophysical Research, v. 102 (C2), p. 3405–3420, doi: 10.1029/96JC03601.

——2006, Flow, hydrography, turbulent mixing, and dissipation at Fieberling Guyot examined with a primitive equation model: Journal of Geophysical Research, v. 111, C07014, doi:10.1029/2005JC003224.

Lavelle, J.W., and Mohn, C., 2010, Motion, commotion, and biophysical connections at deep ocean seamounts: Oceanography, v. 23(1), p. 90–103, doi: 10.5670/oceanog.2010.64.

Lavelle, J.W., Baker, E.T., and Cannon, G.A., 2003, Ocean currents at Axial Volcano, a northeastern Pacific seamount: Journal of Geophysical Research, v. 108(C2), article 3020, doi:10.1029/2002JC001305.

Lavelle, J.W., Massoth, G.J., Baker, E.T., and de Ronde, C.E.J., 2008, Ocean current and temperature time series at Brothers volcano: Journal of Geophysical Research, v. 113, doi:10:1029/2007JC004713.

Lee, H.J., Seo, J.H, de Ronde, C.E.J., and Heinrich, C.H., in press, Fluid inclusion evidence for subseafloor magmatic-hydrothermal processes at Brothers volcano, Kermadec arc, New Zealand: Economic Geology.

Lupton, J.E., 1995, Hydrothermal plumes: Near and far field: American Geophysical Union, Geophysical Monograph 91, p. 317–346, doi: 10.1029/GM091p0317.

Massoth, G.J., de Ronde, C.E.J., Lupton, J.E., Feely, R.A., Baker, E.T., Lebon, G.T., and Maenner, S.M., 2003, Chemically rich and diverse submarine hydrothermal plumes of the southern Kermadec volcanic arc (New Zealand): Geological Society of London, Special Publication 219, p. 119–139.

McDougall, T.J., 1990, Bulk properties of "hot smoker" plumes: Earth and Planetary Science Letters, v. 99, p. 185–194.

Neuholz, R., Schnetger, B., Kleint, C., Koschinsky, A., Letternamm, K., Sander, S., Türke, A., Walter, M., Zitoun, R., and Brumsack, H-J., 2020, Near-field hydrothermal plume dynamics at Brothers volcano (Kermadec arc): A short-lived radium isotope study: Chemical Geology, v. 533, article 119379, doi: 10.1016/j.chemgeo.2019.119379.

Reysenbach, A.L., St. John, E., Meneghin, J., Flores, G.E., Podar, M., Dombrowski, N., Spang, A., L'Haridon, S., Humphris, S.E., de Ronde, C.E.J., Caratori Tontini, F., Tivey, M., Stucker, V.K., Stewart, L.C., Diehl, A., and Bach, W., 2020, Complex subsurface hydrothermal fluid mixing at a submarine arc volcano supports distinct and highly diverse microbial communities: Proceedings of the National Academy of Sciences (PNAS), v. 117(51), p. 32,627–32,638, doi: 10.1073/pnas.2019021117.

Roemmich, D., and Sutton, P., 1998, The mean and variability of ocean circulation past northern New Zealand: Determining the representativeness of hydrographic climatologies: Journal of Geophysical Research, v. 103(C6), p. 13,041–13,054.

Stanton, B.R., 2002, Antarctic intermediate water variability in the northern New Zealand region: New Zealand Journal of Marine and Freshwater Research, v. 36(3), p. 645–654, doi: 10.1080/00288330.2002.9517120.

Staudigel, H., Hart, S.R., Koppers, A.A.P., Constable, C., Workman, R., Kurz, M., and Baker, E.T., 2004, Hydrothermal venting at Vailulu'u Seamount: The smoking end of the Samoan chain: Geochemistry, Geophysics, Geosystems, v. 5, Q02003, doi: 10.1029/2003GC000626.

Stoffers, P., Wright, I.C., de Ronde, C.E.J., Hannington, M.J., Villinger, H., Herzig, P., and the Shipboard Party, 1999, Little studied arc-backarc system in the spotlight: EOS, Transactions of the American Geophysical Union, v. 80, p. 353 and 359.

Stott, M.B., Saito, J.A., Crowe, M.A., Dunfield, P.F., Hou, S., Nakasone, E., Daughney, C.J., Smirnova, A.V., Mountain, B.W., Takai, K., and Alam, M., 2008, Culture-independent characterization of a novel microbial community at a hydrothermal vent at Brothers volcano, Kermadec arc, New Zealand: Journal of Geophysical Research, v. 113, B08S06, doi: 10.1029/2007JB005477

Stucker, V.K., de Ronde, C.E.J., Laurence, K.J., and Phillips, A.M., in press, Rare time series of hydrothermal fluids for a submarine volcano: 14 years of vent fluid compositions for Brothers volcano, Kermadec arc, New Zealand: Economic Geology.

Sutton, P.J.H., and Chereskin, T.K., 2002, Absolute geostrophic currents in the East Auckland Current region: New Zealand Journal of Marine and Freshwater Research, v. 36, p. 4751–4762, doi: 10.1080/00288330.2002.9517128.

Takai, K., Nunoura, T., Horikoshi, K., Shibuya, T., Nakamura, K., Suzuki, Y., Stott, M., Massoth, G.J., Christenson, B.W., de Ronde, C.E.J., Butterfield, D.A., Ishibashi, J-I, Lupton, J.E., and Evans, L.J., 2009, Variability in microbial communities in black smoker chimneys at the NW Caldera vent field, Brothers volcano, Kermadec arc: Geomicrobiology Journal, v. 26(8), p. 552–569, doi: 10.1080/01490450903304949.

Walker, S.L., Baker, E.T., Resing, J.A., Nakamura, K., and McLain, P.D., 2007, A new tool for detecting hydrothermal plumes: An ORP sensor for the PMEL MAPR: EOS, Transactions of the American Geophysical Union, v. 88(52), Fall Meeting Supplement, Abstract V21D-0753.

Wright, I.C., de Ronde, C.E.J., Faure, K., and Gamble, J.A., 1998, Discovery of hydrothermal sulfide mineralization from southern Kermadec arc volcanoes (SW Pacific): Earth and Planetary Science Letters, v. 164, p. 335–343.

Xu, G., and Lavelle, J.W., 2017, Circulation, hydrography, and transport over the summit of Axial Seamount, a deep volcano in the Northeast Pacific: Journal of Geophysical Research: Oceans, v. 122, p. 5404–5422, doi: 10.1002/2016JC012464.

Sharon Walker is an oceanographer at NOAA's Pacific Marine Environmental Laboratory in Seattle, Washington. An original member of the NOAA Vents (now Earth-Ocean Interactions) program, she specializes in developing methods and instrumentation for detecting, monitoring, and mapping hydrothermal plumes at midocean ridges, submarine volcanoes, and volcanic lakes. These methods are also used to characterize chemosynthetic ecosystems at sea-floor methane seeps. Other areas of study include the dispersal of fine ash into the deep ocean from actively erupting submarine volcanoes. She has participated in numerous research expeditions since 1979, including several to the submarine volcanoes of the Mariana, Kermadec, Tofua, and Aeolian arcs.